J|A|C|S COMMUNICATIONS

Published on Web 12/02/2010

Detecting the "Afterglow" of ^{13}C NMR in Proteins Using Multiple Receivers

Ēriks Kupče,*,† Lewis E. Kay,‡ and Ray Freeman§

Agilent Technologies, 6 Mead Road, Yarnton, Oxford OX5 1QU, U.K., Departments of Molecular Genetics, Biochemisty, and Chemistry, University of Toronto, Toronto, Ontario, Canada M5S 1A8, and Jesus College, Cambridge University, Cambridge CB5 8BL, U.K.

Received September 5, 2010; E-mail: eriks.kupce@agilent.com

Abstract: We show that the weak signal that remains after ^{13}C-detected experiments (the ^{13}C "afterglow") can still be measured with high sensitivity by proton detection. This is illustrated by the incorporation of two experiments, 2D (HA)CACO and 3D (HA)CA-(CO)NNH, into a single pulse sequence that makes use of two receivers in parallel. In cases where the sensitivity is not limiting, such as applications to small proteins, the inclusion of the projection−reconstruction method permits the recording of both spectra in only 15 min. High-quality data sets for the 143 residue nuclease A inhibitor (2 °C, correlation time 17.5 ns) were obtained in 3 h, illustrating the utility of the method even in studies of moderately sized proteins.

Parallel acquisition of NMR spectra from nuclei such as ^{1}H, ^{13}C, ^{15}N, ^{19}F, and ^{31}P offers significant economies of instrument time,[1,2] and more importantly, it permits the incorporation of several standard pulse sequences such as HSQC, HMBC, and INADEQUATE into a single entity with the goal of increasing the information content of an NMR experiment. In some cases, this can provide the complete structure of a small molecule from a single measurement.[3,4] These innovations rely on recent instrumental developments that employ two or more receivers operating in parallel. It is shown here that the same principles can be extended to NMR spectroscopy of biomolecules, such as RNA and proteins.

Biochemical samples present new challenges for the parallel acquisition schemes that were originally designed to work with the low natural isotopic abundances of ^{13}C and ^{15}N. In protein research, there is considerable interest in *direct* detection of the low-γ nuclei ^{15}N or ^{13}C,[5] partly because they are less susceptible than protons to broadening by paramagnetic species. One such carbon direct-detection experiment is two-dimensional (2D) (HA)CACO, in which Cα and CO chemical shifts are recorded in F_1 and F_2, respectively.[6] We show here that it is possible to record such a data set with high sensitivity and at the same time measure a three-dimensional (3D) spectrum—in this case an (HA)CA(CO)NNH data set[7] (see below)—with essentially no penalty in measurement time by exploiting multiple receiver technology and a pulse scheme that has been adapted to deal with globally enriched protein samples.

In principle, the most attractive procedure in a multireceiver-based experiment might be to start with detection of the least sensitive species, such as ^{15}N, then transfer the remaining magnetization to a more sensitive species (e.g., ^{13}C) for further detection, and finish the observations on the most sensitive nuclei, protons. In practice, the illustrative example presented here starts by detecting ^{13}C in the 2D (HA)CACO experiment[6] (Figure 1, black). The ^{13}C signals are directly detected at the acquisition stage but also leave an "afterglow", i.e., the very weak magnetization at the extreme tail of the truncated free induction signal that has decayed too far for direct ^{13}C detection. While under normal circumstances the experiment would stop at this point, in the present case, this small fraction of magnetization is retrieved, refocused, and transferred to protons (Figure 1, red) to exploit the advantageous proton sensitivity. In the present application, the "left-over" ^{13}C signal, corresponding to ∼10% of that originating on CO at the start of the detection period for 2D (HA)CACO, is used for the 3D (HA)CA(CO)NNH experiment. The 3D spectrum is thus obtained in parallel with the desired 2D data set, and as we discuss below, this additional information is obtained with essentially no penalty in spectrometer time.

Figure 1 illustrates the combined dual-receiver 2D (HA)CACO (black)/3D (HA)CA(CO)NNH (black + red) experiment, with the latter recorded in an enhanced sensitivity mode.[8,9] The magnetization flow during the 2D and 3D experiments can be summarized as follows:

$$^{1}\mathrm{H}\alpha \xrightarrow{J_{\mathrm{HC}}} {}^{13}\mathrm{C}\alpha, t_1 \xrightarrow{J_{\mathrm{C}\alpha\mathrm{CO}}} {}^{13}\mathrm{CO}, t_2$$

$$^{1}\mathrm{H}\alpha \xrightarrow{J_{\mathrm{HC}}} {}^{13}\mathrm{C}\alpha, t_1 \xrightarrow{J_{\mathrm{C}\alpha\mathrm{CO}}} {}^{13}\mathrm{CO} \xrightarrow{J_{\mathrm{CON}}} {}^{15}\mathrm{N}, t_2 \xrightarrow{J_{\mathrm{HN}}} {}^{1}\mathrm{H}^{\mathrm{N}}, t_3$$

where the active coupling responsible for each transfer step is indicated above the corresponding arrow and the t_i ($i = 1, 2, 3$) are evolution times.

The 2D (HA)CACO experiment starts with an INEPT[13] polarization transfer from Hα protons to the Cα carbon site (Figure 1, black). This is followed by an evolution period t_1 and coherence transfer from Cα to CO with simultaneous decoupling of ^{1}H, Cβ, and ^{15}N. Once the magnetization arrives at the CO site, it is antiphase with respect to Cα. The antiphase magnetization can be recorded with a second receiver during t_2' and the antiphase doublet peaks "collapsed" to a singlet by deconvolution in a postacquisition manner.[14] Alternatively, as is done in the applications described here (see below), the IPAP scheme[15] can be used for the same purpose, except that the antiphase CO magnetization $\mathrm{CO}_Y\mathrm{C}\alpha_Z$ is refocused into CO_X (panel A of Figure 1) or left in the antiphase state (panel B) before it is detected during t_2'. Subsequent postacquisition manipulation of the data produces the desired CO "decoupled" spectrum in F_2' (see the Figure 2 caption). It should be noted that under normal circumstances the IPAP feature would have required two separate experiments, one for each of sequences A and B. However, schemes A and B in the present case are subsumed into the two data sets that are recorded for F_2 (^{15}N) quadrature detection in the 3D experiment, resulting in a savings in time by a factor of 2. Thus, for each t_2 point, a pair of data sets

† Agilent Technologies.
‡ University of Toronto.
§ Cambridge University.

10.1021/ja1080025

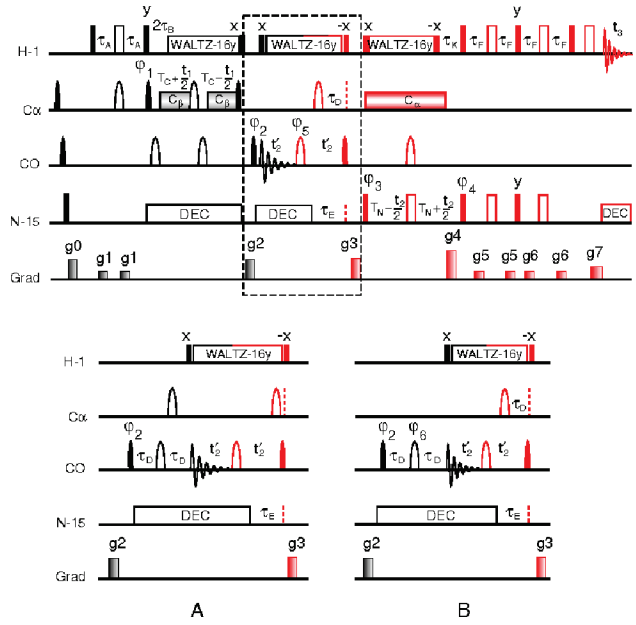

Figure 1. The combined dual-receiver 2D (HA)CACO (black)/3D (HA)CA(CO)NNH (black + red) experiment. The antiphase doublet CO peaks in F_2' (due to an active coupling to Cα) can be "collapsed" to a singlet by deconvolution in a postacquisition manner.[14] Alternatively, the dashed box is replaced by panels A and B, which show the IPAP versions[15] of the pulse sequence. All filled (open) pulses have a tip angle of 90° (180°). The shaped ^{13}Cα and ^{13}CO pulses are applied at field strengths of $\Delta/\sqrt{15}$ and $\Delta/\sqrt{3}$ for 90 and 180° tip angles, respectively, where Δ is the distance in Hz between the centers of the ^{13}Cα and ^{13}CO spectral windows. ^{13}Cβ decoupling during t_1 was achieved using a constant adiabaticity WURST-8 decoupling scheme[18] with a bandwidth of 25 ppm centered at 27.5 ppm (swept from 15 to 40 ppm). An additional equivalent field swept from 101 to 76 (centered at 88.5 ppm) was applied as well; this essentially eliminates decoupling artifacts that would otherwise be manifested when only a single field centered at 27.5 ppm is applied.[19] The B_{1max} (B_{1rms}) of the combined decoupling fields was 0.84 (0.48) kHz (600 MHz). ^{13}Cα decoupling during t_2 employed a 3.84 kHz, 118 ppm cosine-modulated SEDUCE-1 decoupling scheme.[20] Delays: $\tau_A = 1.7$ ms, $\tau_B = 1.8$ ms, $\tau_D = 4.625$ ms, $\tau_E = 24$ ms, $\tau_F = 2.3$ ms, $\tau_K = 5.5$ ms, $T_C = 4$ ms, $T_N = 12.4$ ms. The acquisition times for the directly detected free induction decays of ^{13}C and ^{1}H nuclei, t_2' and t_3, were set to 42.6 ms, and 512 complex data points were acquired on both receivers. Phase cycling: $\varphi_1 = x, -x$; $\varphi_2 = 2(x), 2(-x)$; $\varphi_3 = 4(x), 4(-x)$; $\varphi_4 = x$; ^{13}C receiver $= x, -x, -x, x$; ^{1}H receiver $= x, -x, -x, x, -x, x, x, -x$. Phases φ_5 (top scheme) and φ_6 (scheme B) are adjusted to compensate for the Bloch−Siegert effects introduced by the Cα pulse. It should be noted that all of the data sets in the present study were acquired with two transients, and hence, only the first two steps of the phase cycle were employed. Quadrature detection in F_1 was achieved by incrementing φ_1 by 90°.[17] Quadrature detection in F_2 was achieved by recording a pair of data sets for each t_2 point with (g_4, φ_4) and ($-g_4$, $-\varphi_4$).[8,9] In the case where the IPAP scheme is used, sequence A is implemented for (g_4, φ_4) and scheme B for ($-g_4$, $-\varphi_4$), thereby reducing the experiment time by a factor of 2. Gradient strengths (G/cm) and durations (ms): $g_0 = (10, 0.5)$, $g_1 = (8, 0.5)$, $g_2 = (20, 1)$, $g_3 = (-15, 1)$, $g_4 = (30, 1.25)$, $g_5 = (3, 0.3)$, $g_6 = (2.5, 0.4)$, $g_7 = (29.5, 0.125)$.

is recorded corresponding to (scheme A, g_4, φ_4) and (scheme B, $-g_4$, $-\varphi_4$). These data sets can be manipulated in the usual way[8] to produce an enhanced-sensitivity 3D Cα−N−H^N correlation map. They can also be manipulated to improve the sensitivity of the 2D (HA)CACO spectrum by recognizing that 2D (t_1, t_2') data sets are unaffected by the portion of the pulse sequence that follows the t_2' period (CO direct detection). The sensitivity of each (t_1, t_2') plane can therefore be enhanced by summing over all t_2 (^{15}N) points obtained with scheme A (corresponding to in-phase CO detection during t_2'), with a second corresponding time-domain data set obtained by repeating the process with data from scheme B (antiphase CO detection). These two "summed" maps are then the

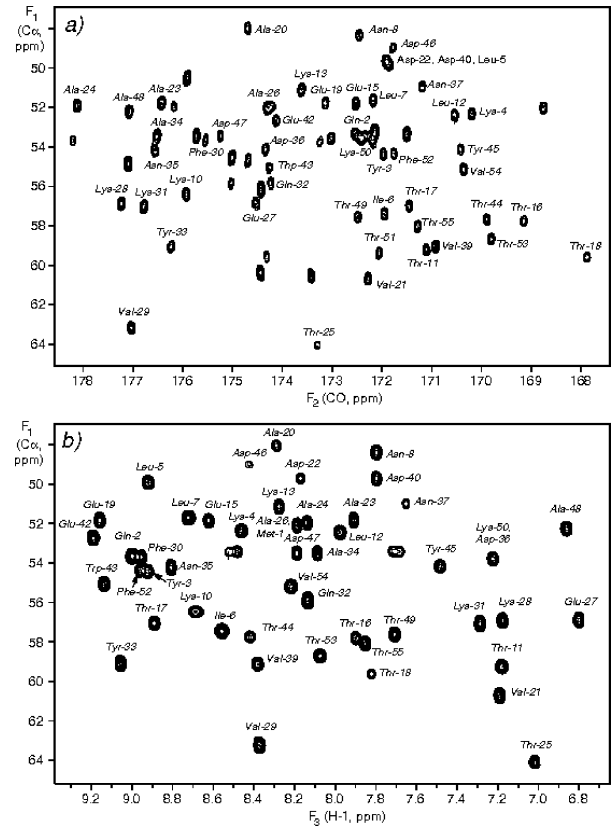

Figure 2. (a) The ^{13}C-detected 2D (HA)CACO spectrum of a 1.0 mM aqueous solution of GB1 (90% H_2O, 10% D_2O) recorded in parallel with (b) the ^{1}H-detected 3D (HA)CA(CO)NNH experiment, obtained in 190 min. Panel (b) shows the F_1F_3 projection of the 3D experiment. The spectral widths in (a) were 3 kHz (F_1) and 12 kHz (F_2), and those in (b) were 3 kHz (F_1), 2 kHz (F_2), and 12 kHz (F_3). In panel (a), 24 (F_1) and 512 (F_2) complex points were recorded; in (b), 24 (F_1), 50 (F_2), and 512 (F_3) complex points were recorded. Following acquisition, the data sets were separated, and the data sizes in the directly detected dimensions (t_2', t_3) were further reduced by a factor of 4 (or the nearest available power of two) by retaining only the active spectral bandwidths of interest. The data matrices were then zero-filled to 128 × 512 and 128 × 256 × 512 complex points and processed using linear prediction in the indirectly detected dimensions. The IPAP spectra were processed by calculating sums and differences for the series of pairs of planes recorded in parallel with the 3D experiment. A further $\sqrt{2}$ advantage in sensitivity is obtained by adding these spectra together (after frequency shifting in F_2' by ±26.5 Hz) to produce the final (HA)CACO spectrum. If the IPAP step is not selected, the $J_{C\alpha CO}$ couplings can be deconvoluted as described previously.[14] The unassigned peaks are due to impurities.

IPAP pair that is recombined in the usual way[15] to generate the 2D (HA)CACO spectrum (see the Figure 2 caption). This ability to intertwine elements of the 2D scheme within the framework of the 3D experiment, as illustrated here, is just one of the practical advantages of having more than one basic pulse sequence within a single entity. Importantly, it allows signal averaging to be performed for 2D (HA)CACO by manipulation of parts of the 3D data set (summing over the t_2 data, see above), which means that there is effectively no penalty for recording the 3D spectrum.

The key to all parallel acquisition sequences is to use all of the available magnetization components to the best advantage. The 3D experiment shares the first t_1 evolution stage involving Cα with the 2D data set. Once the 2D (HA)CACO experiment has been acquired, CO chemical shift evolution from the first t_2' period is refocused during a second t_2' delay. ^{15}N decoupling is switched off during τ_E (Figure 1) to allow the evolution of CO magnetization due to the $^{1}J_{CON}$ coupling, and a 180° pulse on Cα ensures that

evolution from the $^1J_{COC\alpha}$ coupling occurs for a period of $2\tau_D$, refocusing $CO_YC\alpha_Z$. The CO refocusing pulse (phase φ_5, top sequence of Figure 1 or phase φ_6, scheme B) compensates for the Bloch−Siegert effects introduced by the Cα pulse.[16] In contrast, in scheme A a pair of Cα 180° pulses is applied on opposite sides of the second CO refocusing pulse, eliminating the need for any phase adjustment. The antiphase CO magnetization, CO_YN_Z, is subsequently transferred to ^{15}N, and a second evolution period t_2 encodes this ^{15}N magnetization during a constant-time interval incorporated into the ^{15}N−CO refocusing delay. This magnetization is then transferred to the protons for detection.

As a first test of the methodology, a 1 mM sample of the protein GB1 (54 residues) globally enriched in ^{13}C and ^{15}N was studied on a Varian 600 MHz spectrometer equipped with a proton−carbon−nitrogen probe with cryogenically cooled ^{13}C and ^{1}H receiver coils and preamplifiers. The carbon-detected 2D (HA)CA-CO spectrum and the proton-detected 3D (HA)CA(CO)NNH spectrum (the latter displayed as a projection on the F_1F_3 plane) are shown in Figure 2a,b, respectively. These two data sets were recorded in parallel as described above in a total measurement time of slightly more than 3 h.

Combination of the two- and three-dimensional elements implies some compromise. There is interplay between the resolution in the directly recorded ^{13}C spectrum of the 2D stage and the sensitivity achieved in the proton spectrum of the 3D stage (the Supporting Information shows a calculation of the optimum truncation point of a free induction decay that yields the highest signal-to-noise ratio). Longer ^{13}C free induction decays leave less magnetization for transfer to protons. In practice, the ^{13}C acquisition time was limited to 42 ms for the application to GB1, leaving a sufficiently strong proton signal. The ^{13}C resolution could be improved by increasing the acquisition time, but this would be accompanied by the danger that proton signals associated with broader CO sites might be lost. In applications to higher-molecular-weight proteins, where relaxation effects are more severe, the t_2' period would be shortened appropriately to preserve enough signal for the subsequent steps in the 3D experiment. An example of such a case is discussed below and in the the Supporting Information.

The speed of the measurements was further increased by the projection−reconstruction (PR) technique, which uses the Fourier transform of a small set of radially sampled time-domain signals followed by 3D reconstruction.[10−12] A 3D spectrum was reconstructed from projections onto just three planes: the orthogonal "first planes" F_1F_3 ($t_2 = 0$; 2 min acquisition time) and F_2F_3 ($t_1 = 0$; 4 min) and a tilted plane rotated about the F_3 axis from F_1 toward F_2 through an angle $\delta = 69.5°$. This particular inclination was chosen by numerical optimization and lies closer to F_2 (^{15}N) to take advantage of the narrower lines and better shift dispersion of ^{15}N relative to ^{13}Cα. The tilted experiment employed 56 increments in the jointly sampled time dimension and was completed in 9 min.

Figure 3a shows the F_2F_3 plane at $F_1 = 51.93$ ppm (correlating the nitrogen and proton shifts) obtained from the conventional data set recorded with (24, 50) complex (t_1, t_2) data points in a duration of 190 min using the IPAP scheme of Figure 1A,B. The resulting F_2F_3 projection (Figure 3b) from the PR data set compares very well with the conventional result shown in Figure 3a, despite the fact that it was recorded in 1/12 the measurement time.

As described above, the 3D PR (HA)CA(CO)NNH spectrum was reconstructed from three planes, including a single tilted projection. The ^{13}C-detected (HA)CACO 2D spectrum is readily obtained from PR data using just the tilted plane. Here it is important to note that this plane is obtained by incrementing (t_1, t_2) according to (cos δ) /sw_{tilt} and (sin δ)/sw_{tilt}, where sw_{tilt} is the spectral width in the indirectly

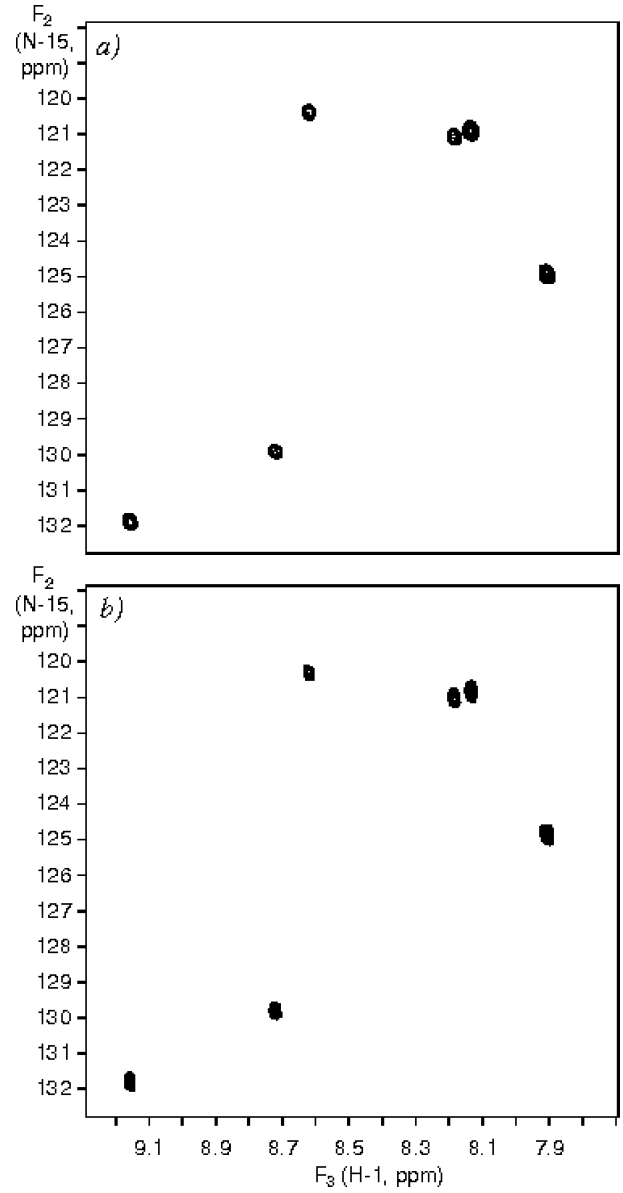

Figure 3. Comparison between the F_2F_3 planes at $F_1 = 51.93$ ppm of (a) the conventional 3D (HA)CA(CO)NNH spectrum of GB1 recorded in 190 min (see the Figure 2 caption) and (b) the reconstructed 3D spectrum recorded using the PR technique in just 15 min. The optimum projection angle of 69.5° was used to record the tilted plane in parallel with the ^{13}C-detected (HA)CACO experiment (see the Supporting Information).

detected dimension that combines ^{15}N and ^{13}Cα chemical shifts (δ = 69.5°).[10−12] Since magnetization that is detected during t_2' does not depend on subsequent steps in the sequence, it is clear that peaks in the reconstructed (HA)CACO spectrum will appear at frequencies $\omega_{C\alpha}$ cos δ in the F_1 dimension. Thus, the "correct" frequency, $\omega_{C\alpha}$, is restored by scaling the F_1 axis by a factor of (cos δ)$^{-1}$, as shown in the Supporting Information. The PR approach employs the very same IPAP strategy as the full Cartesian sampling method; a factor of 2 in time is saved by incorporating schemes A and B into the two data sets required for F_2 quadrature detection. It should be noted that in the PR approach, the (HA)CA(CO)NNH spectrum is obtained *in parallel* with the IPAP version of the (HA)CACO spectrum, just as for the data set recorded in 3 h where Cα and ^{15}N are sampled conventionally (i.e., where reconstruction is not required).

The experimental results described above provide a "proof-of-principle" of the utility of a dual-receiver approach for recording

simultaneous data sets on small uniformly ^{15}N,^{13}C-labeled protein samples. As a further test of the methodology, we recorded combined (HA)CACO/(HA)CA(CO)NNH spectra of a larger protein, the nuclease A inhibitor (NuiA, 143 amino acids) at both 25 and 2 °C using the IPAP scheme described above with a 24 ms ($t_2'_{max}$) CO acquisition time and total measurement times of 3 h per experiment (1 mM protein concentration). ^{15}N spin relaxation experiments[21] have established that NuiA tumbles with effective correlation times of 8.8 ± 0.6 and 17.5 ± 1.2 ns at these temperatures. The sensitivity of (HA)CACO decreases by a factor of ~2 from 25 to 2 °C (average signal-to-noise of peaks = 107:52 at the two temperatures), while a larger drop is noted for the 3D experiment (112:18) that reflects the larger number of transfer steps, including the second t_2' period that is necessary for refocusing the CO chemical shift that was recorded with the second receiver in (HA)CACO (see Figure 1). Despite these sensitivity losses, essentially all of the correlations that were observed at 25 °C were also noted at 2 °C, indicating that the dual-receiver experiment has utility for moderately sized proteins as well.

These results demonstrate that the original parallel-acquisition protocol[1−4] can be successfully extended to experiments on biomolecules globally enriched in ^{13}C and ^{15}N. A pulse sequence combining a 2D ^{13}C-detected experiment with a 3D proton-detected measurement has been designed. For small to moderately-sized proteins at millimolar concentrations, simultaneous (HA)CACO and (HA)CA(CO)NNH data sets can be recorded in only a few hours with an experiment that exploits ^{13}CO and $^{1}H^{N}$ direct acquisition using a pair of receivers. In cases where sensitivity is not limiting, the measurement time can be further substantially reduced with projection−reconstruction techniques. In the illustrative example reported here, both 2D and 3D spectra were recorded on the 54 residue protein GB1 in a single measurement lasting only 15 min.

Acknowledgment. The sample of GB1 was kindly provided by Professor Fuyuhiko Inagaki of Hokkaido University. The sample of NuiA was kindly provided by Dr. Robert E. London of the National Institute of Environmental Health Sciences. The authors acknowledge fruitful discussions with Dr. Flemming Hansen. Dr. Ranjith Muhandiram is thanked for analysis of the NuiA ^{15}N relaxation data. This work was supported by a grant from the Natural Sciences and Engineering Research Council of Canada to L.E.K. L.E.K. holds a Canada Research Chair in Biochemistry.

Supporting Information Available: A calculation demonstrating that truncation of a free induction signal at 1.26 times the decay time constant delivers the optimum signal-to-noise ratio whatever the relative level of the noise; a demonstration that the ^{13}C afterglow can be significantly enhanced by magnetization transfer to protons; a figure showing a 2D ^{13}C-detected (HA)CACO spectrum obtained in parallel with the 3D PR experiment; and figures illustrating the applicability of the method to larger proteins. This material is available free of charge via the Internet at http://pubs.acs.org.

References

(1) Kupče, Ē.; Freeman, R.; John, B. K. *J. Am. Chem. Soc.* **2006**, *128*, 9606.
(2) Kupče, Ē.; Cheatham, S.; Freeman, R. *Magn. Reson. Chem.* **2007**, *45*, 378.
(3) Kupče, Ē.; Freeman, R. *J. Am. Chem. Soc.* **2008**, *130*, 10788.
(4) Kupče, Ē.; Freeman, R. *Magn. Reson. Chem.* **2010**, *48*, 333.
(5) Bermel, W.; Bertini, I.; Felli, I. C.; Piccioli, M.; Pierattelli, R. *Prog. NMR Spectrosc.* **2006**, *48*, 25.
(6) Kay, L. E.; Ikura, M.; Tschudin, R.; Bax, A. *J. Magn. Reson.* **1990**, *89*, 496.
(7) Grzesiek, S.; Bax, A. *J. Biomol. NMR* **1993**, *3*, 185.
(8) Kay, L. E.; Keifer, P.; Saarinen, T. *J. Am. Chem. Soc.* **1992**, *114*, 10663.
(9) Schleucher, J.; Sattler, M.; Griesinger, C. *Angew. Chem., Int. Ed. Engl.* **1993**, *32*, 1489.
(10) Freeman, R.; Kupče, Ē. *J. Biomol. NMR* **2003**, *27*, 101.
(11) Kupče, Ē.; Freeman, R. *J. Biomol. NMR* **2003**, *27*, 383.
(12) Kupče, Ē.; Freeman, R. *J. Am. Chem. Soc.* **2004**, *126*, 6429.
(13) Morris, G. A.; Freeman, R. *J. Am. Chem. Soc.* **1979**, *101*, 760.
(14) Le Parco, J. M.; McIntyre, L.; Freeman, R. *J. Magn. Reson.* **1993**, *97*, 533.
(15) Yang, D.; Nagayama, K. *J. Magn. Reson., Ser. A* **1996**, *118*, 117. Ottiger, M.; Delaglio, F.; Bax, A. *J. Magn. Reson.* **1998**, *131*, 373.
(16) Vuister, G. W.; Bax, A. *J. Magn. Reson.* **1992**, *98*, 428.
(17) Marion, D.; Ikura, M.; Tschudin, R.; Bax, A. *J. Magn. Reson.* **1989**, *85*, 393. States, D. J.; Haberkorn, R. A.; Ruben, D. J. *J. Magn. Reson.* **1982**, *48*, 286. Drobny, G.; Pines, A.; Sinton, S.; Weitekamp, D. P.; Wemmer, D. *Faraday Symp. Chem. Soc.* **1978**, 13.
(18) Kupče, Ē.; Freeman, R. *J. Magn. Reson., Ser. A* **1996**, *118*, 299.
(19) Zhang, S.; Gorenstein, D. G. *J. Magn. Reson.* **1998**, *132*, 81.
(20) McCoy, M. A.; Mueller, L. *J. Am. Chem. Soc.* **1992**, *114*, 2108.
(21) Farrow, N. A.; Muhandiram, R.; Singer, A. U.; Pascal, S. M.; Kay, C. M.; Gish, G.; Shoelson, S. E.; Pawson, T.; Forman-Kay, J. D.; Kay, L. E. *Biochemistry* **1994**, *33*, 5984.

JA1080025